

Polyol synthesis of palladium hydride: bulk powders vs. nanocrystals†

Ting-Hao Phan and Raymond E. Schaak*

Received (in Berkeley, CA, USA) 30th January 2009, Accepted 8th April 2009

First published as an Advance Article on the web 1st May 2009

DOI: 10.1039/b902024a

Palladium is converted into palladium hydride, β -PdH_x, in polyol solution using NaBH₄ as a hydrogen source; nanocrystalline Pd reacts to form PdH_x faster and at lower temperatures than bulk Pd, and can be made to release hydrogen to regenerate Pd.

Palladium hydride, PdH_x, is a well-studied prototype material for hydrogen-based fuel systems. Because Pd readily dissociates H₂ and absorbs hydrogen into its lattice, it can function as a hydrogen storage material,¹ a hydrogen dissociation catalyst for activation of other hydrogen storage materials,² and a hydrogen-permeable membrane for transport, separation, and purification.³ PdH_x is also interesting for its composition-dependent superconducting properties,⁴ as well as its applications in sensing and catalysis.⁵ PdH_x most commonly exists in two forms: α -PdH_x (fcc, 0 < x < 0.02) and β -PdH_x (fcc, 0.58 < x < 1),⁶ although γ -PdH_x (tetragonal, x = 1.33) has also been claimed to form by ion implantation.⁷ Palladium hydrides are typically formed by gas-phase hydrogen absorption, high-pressure hydrogen insertion, and electrochemical reactions with palladium.^{1,8} Solution chemistry methods can also produce PdH_x, for example during the aqueous reduction of Pd²⁺ at 100 °C.⁹

An alternative and mild solution chemistry method, introduced by Murphy *et al.*, is to react bulk Pd, as well as bulk-scale hydrogen-absorbing intermetallic compounds, with aqueous borohydride to form hydrides.¹⁰ This study very effectively demonstrated the versatility and generality of low-temperature ambient-pressure chemical methods for hydrogen insertion into metals and intermetallics. While this earlier work focused on bulk-scale materials, applying the borohydride method to nanoscale metals and intermetallics, with PdH_x as a prototype system, is intriguing. For example, nanoscale hydrides are known to have faster reaction kinetics and lower desorption temperatures and activation energies than their bulk analogs,^{1b,11} as well as size-dependent hydrogen contents.¹² Also, non-equilibrium phases can be stabilized in nanocrystalline solids prepared through low-temperature solution routes,¹³ which suggests that similar approaches for hydrides could lead to the discovery of new hydrogen storage materials. In this work, we describe a facile polyol-based chemical route for converting Pd powders and nanocrystals into PdH_x, experimentally demonstrating ambient-pressure solution-phase hydrogen absorption, storage, and release in a prototype metal hydride system. This study effectively

merges the polyol process, one of the more desirable chemical methods for nanocrystal synthesis,¹⁴ with metal hydrides for applications in hydrogen storage.

In a typical synthesis, bulk PdH_x powder was formed by dispersing 20 mg of commercially-available submicron Pd powder (0.25–0.55 μ m, Alfa-Aesar) in 20 mL tetraethylene glycol (TEG), followed by heating to 90–210 °C and then adding 3 mL of a fresh solution of NaBH₄ in TEG (0.4 M) with stirring for 2 min. Pd nanocrystals¹⁵ were synthesized by simultaneously injecting separate ethylene glycol (EG) solutions of Na₂PdCl₄ (3.3 mL, 0.14 M) and poly(vinylpyrrolidone) (PVP, MW = 55 000; 3.3 mL, 0.21 M) into 7 mL of hot EG (typically 110 °C). The Pd nanocrystals were isolated, washed, and re-dispersed in TEG along with additional PVP, and this solution was injected into heated TEG at 90–190 °C, followed by 3 mL of a 0.4 M TEG solution of NaBH₄.

Fig. 1 shows powder X-ray diffraction (XRD) data for bulk (0.25–0.55 μ m) and nanocrystalline (6–15 nm) Pd reacted with NaBH₄ in TEG for 2 min at different temperatures. The bulk and nanocrystalline Pd samples were both found to have lattice constants of a = 3.89 Å, which matches the literature values.¹⁶ It is known that α -PdH_x has a \approx 3.895 Å and β -PdH_x has a \approx 4.025 Å, with concentration-dependent variation from \sim 4.02 to 4.08 Å.⁶ Because of the composition-dependent lattice expansion, XRD is a useful tool for characterizing the formation of PdH_x. Accordingly, as the reaction temperature increases, the XRD pattern for bulk Pd changes to a multi-phase fcc sample that is consistent with lattice expansion due to hydrogen absorption. A GC with a thermal conductivity detector confirmed the presence of hydrogen in the PdH_x products: after heating bulk PdH_x in a closed

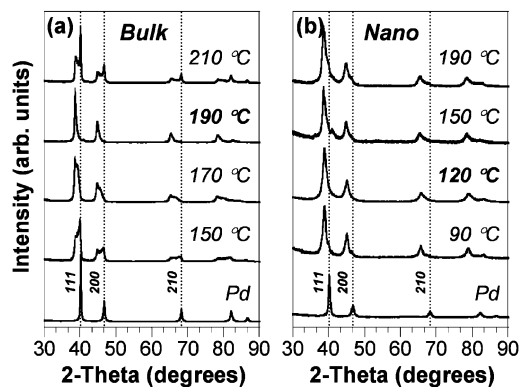


Fig. 1 Powder XRD patterns for (a) bulk Pd and (b) nanocrystalline Pd reacted with NaBH₄ in TEG at the temperatures indicated. Complete conversion to PdH_x occurs at 190 °C for bulk Pd and at 120 °C for nano-Pd. Vertical dashed lines indicate the peak positions for Pd.

Department of Chemistry and Materials Research Institute, The Pennsylvania State University, University Park, PA 16802, USA. E-mail: schaak@chem.psu.edu

† Electronic supplementary information (ESI) available: Complete experimental details and GC data. See DOI: 10.1039/b902024a

system, hydrogen gas was detected in the headspace, while heating bulk Pd under identical closed-system conditions showed no hydrogen. This confirms that the lattice expansion observed by XRD is attributable to hydrogen absorption.

At 190 °C, a nearly phase-pure fcc pattern with $a = 4.040 \text{ \AA}$ is evident. This corresponds to $\beta\text{-PdH}_x$ with $x \approx 0.7$, based on comparison with literature reports.^{6e} Heating to higher temperatures in solution begins to liberate hydrogen, returning the sample to predominantly Pd. Nanocrystalline Pd shows a similar trend, reacting with borohydride under identical conditions to form $\beta\text{-PdH}_x$ ($a = 4.037 \text{ \AA}$), followed by gradual release of hydrogen as the temperature increases. However, most of the nanocrystalline Pd is converted to PdH_x at temperatures as low as 90 °C, with phase-pure PdH_x observed at 120 °C. Thus, nanocrystalline Pd reacts with NaBH_4 in solution to form a hydride at a significantly lower temperature than bulk Pd under otherwise identical reaction conditions.

In addition to forming a hydride at lower temperatures, nanocrystalline PdH_x forms faster in solution than its bulk analog. Fig. 2 shows powder XRD data for the reaction of bulk and nanocrystalline Pd with NaBH_4 in TEG at 90 °C. After 10 min, bulk Pd had begun to absorb hydrogen, as evidenced by the emergence of shoulders to the left of the 111 and 200 peaks of Pd. Based on quantitative analysis of the phase fractions, only 43% of bulk Pd has converted to $\beta\text{-PdH}_x$. After 60 min, slightly more of the sample has been converted to $\beta\text{-PdH}_x$ (54%). However, the reaction is not yet complete, possibly because of decomposition and subsequent lack of availability of the NaBH_4 during the long reaction time. The solution is replenished with a fresh solution of NaBH_4 , and the phase fraction of $\beta\text{-PdH}_x$ again begins to increase, reaching a maximum of 74%. However, conversion to PdH_x is not complete at 90 °C. In contrast, 91% of the nanocrystalline Pd has converted to $\beta\text{-PdH}_x$ after only 1 min of reaction with NaBH_4 in TEG at 90 °C, with almost phase-pure $\beta\text{-PdH}_x$ formed within 10 min.

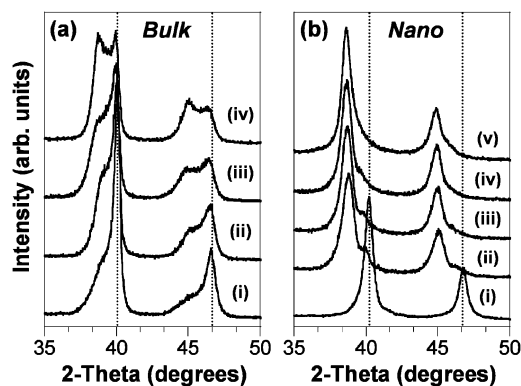


Fig. 2 Powder XRD patterns showing the time-dependent reactivity of (a) bulk Pd and (b) nano-Pd. In (a), bulk Pd was reacted with NaBH_4 in TEG for (i) 10 min and (ii) 60 min, then fresh NaBH_4 was added and reacted for an additional (iii) 10 min and (iv) 60 min. In (b), nanocrystalline Pd (i) was reacted with NaBH_4 in TEG for (ii) 1 min, (iii) 5 min, and (iv) 10 min, then (v) an additional 10 min after adding fresh NaBH_4 . Vertical dashed lines indicate the positions of the 111 and 200 peaks for Pd.

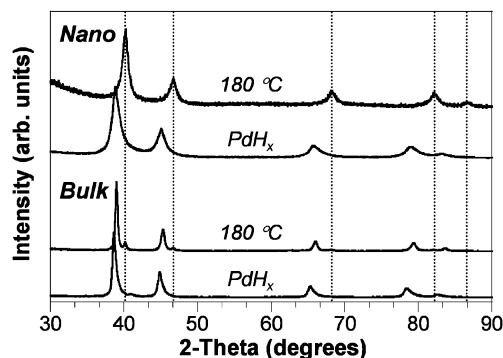


Fig. 3 Powder XRD patterns showing hydrogen release for bulk and nanocrystalline PdH_x . For bulk PdH_x (bottom), heating to 180 °C releases some of the hydrogen, generating PdH_x with a smaller hydrogen content along with some Pd. For nano-Pd (top), heating to 180 °C releases all of the hydrogen, generating only nano-Pd as a product. Vertical dashed lines indicate the peak positions for Pd.

Nanocrystalline PdH_x can also release the hydrogen to re-form Pd at lower temperatures than bulk Pd. Fig. 3 shows powder XRD data for the purest attainable samples of bulk and nanocrystalline PdH_x , as well as these samples heated to 180 °C for 4 h in a tube furnace under Ar. Under these conditions, bulk Pd had begun to release hydrogen to form a PdH_x phase with lower hydrogen content ($a = 4.00 \text{ \AA}$ after heating vs. $a = 4.04 \text{ \AA}$ before heating), as well as a small amount of Pd. In contrast, nanocrystalline PdH_x has released almost all of the hydrogen under these conditions, as indicated by the XRD pattern showing nearly phase-pure Pd without evidence of PdH_x . The hydrogen can also be released in solution by heating to higher temperatures, e.g. 270 °C in 1-octadecene. Differences between PdH_x prepared using traditional methods¹ and those made in polyol solution could arise from some solvent decomposition and subsequent carbon inclusion, either coating the surface or intercalated into the structure, or interstitial boron from the borohydride.

Fig. 4a shows a TEM image and selected area electron diffraction (SAED) pattern for the Pd nanocrystals that were synthesized as described earlier. These nanocrystals were then isolated, washed several times, and re-dispersed in fresh TEG before adding NaBH_4 and heating to 120 °C to form PdH_x . The TEM image in Fig. 4b shows that the resulting PdH_x nanocrystals are similar in size and shape to the Pd nanocrystal precursors. Quantitative analysis of the SAED patterns for PdH_x confirms that the nanocrystals correspond to the hydride: $a = 3.9 \text{ \AA}$ for the Pd nanocrystals in Fig. 4a and $a = 4.1 \text{ \AA}$ for the PdH_x nanocrystals in Fig. 4b.

The general size and morphology of the Pd nanocrystals are retained after absorbing hydrogen to form $\beta\text{-PdH}_x$, as well as after releasing hydrogen to re-form Pd. Fig. 4c shows a TEM image of a sample of Pd nanocrystals and Fig. 4d shows this same sample after conversion to $\beta\text{-PdH}_x$. The nanocrystals remain similar in size and morphology upon heating to 180 °C for 4 h to release the hydrogen and regenerate Pd (Fig. 4e). This indicates that the hydriding and dehydriding reactions can be carried out on pre-formed Pd nanocrystals and proceed with general retention of size and morphology. It is likely that the PVP stabilizer helps to prevent significant aggregation, as

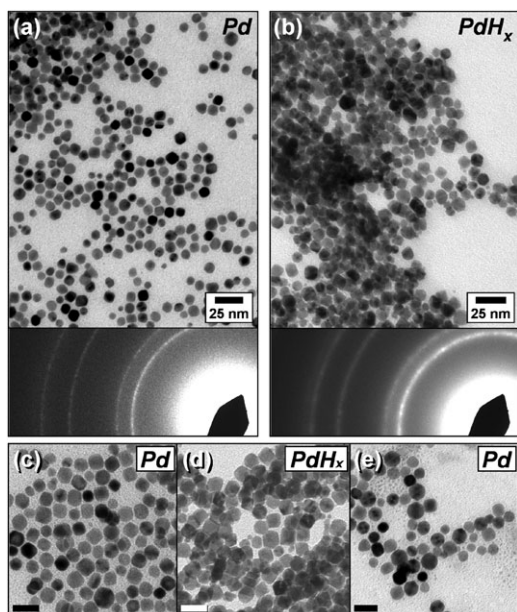


Fig. 4 TEM images and corresponding SAED patterns of (a) Pd nanocrystals and (b) β -PdH_x nanocrystals. The bottom panels show (c) Pd nanocrystals, (d) PdH_x nanocrystals after reaction with NaBH₄ in TEG, and (e) regenerated Pd nanocrystals after hydrogen release. Scale bars in (c), (d), and (e) correspond to 20 nm.

was observed for other nanocrystal systems prepared using similar temperatures.¹⁷

In conclusion, we have demonstrated a facile low-temperature and ambient-pressure solution-phase process for converting bulk and nanocrystalline Pd into β -PdH_x, effectively merging the polyol process for nanocrystal synthesis with metal hydride hydrogen storage materials. The experiments indicate that nanocrystalline Pd absorbs and releases hydrogen faster and at lower temperatures than bulk Pd, and results in the formation of dispersible metal hydride nanocrystals with general size and morphology retention relative to the metal nanoparticle templates. In analogy to similar chemistry in non-hydride systems, other available shapes of Pd nanoparticles, including rods, bars, and plates,¹⁸ should provide access to analogous shapes of PdH_x nanoparticles that would be useful for studying the properties of shape-controlled metal hydride nanocrystals. This chemistry should also be portable to other metal and alloy systems, perhaps opening the door to a library of colloidal metal and intermetallic hydride nanocrystals with hydrogen absorption and release capabilities.

This work was supported by the US Department of Energy (DE-FG02-08ER46483), the Petroleum Research Fund (administered by the American Chemical Society), a DuPont Young Professor Grant, a Beckman Young Investigator Award, a Sloan Research Fellowship, and a Camille Dreyfus Teacher-Scholar Award. Electron microscopy was performed at the Electron Microscopy Facility at the Huck Institutes for the Life Sciences at Penn State. The authors thank Seung-Hyun Anna Lee for help with GC data collection.

Notes and references

- (a) S. Kishore, J. A. Nelson, J. H. Adair and P. C. Eklund, *J. Alloys Compd.*, 2005, **389**, 234; (b) S. Horinouchi, Y. Yamanoi, T. Yonezawa, T. Mouri and H. Nishihara, *Langmuir*, 2006, **22**, 1880; (c) H. Kobayashi, M. Yamauchi, H. Kitagawa, Y. Kubota, K. Kato and M. Takata, *J. Am. Chem. Soc.*, 2008, **130**, 1828; (d) *Hydrogen in metals II*, ed. G. Alefeld, J. Volkl, Springer, Berlin, Heidelberg, 1978.
- (a) M. Sabo, A. Henschel, H. Frode, E. Klemm and S. Kaskel, *J. Mater. Chem.*, 2007, **17**, 3827; (b) X. Shan, J. H. Payer and J. S. Wainright, *J. Alloys Compd.*, 2007, **430**, 262; (c) A. Anson, E. Lafuente, E. Urriolabeitia, R. Navarro, A. M. Benito, W. K. Maser and M. T. Martinez, *J. Phys. Chem. B*, 2006, **110**, 6643.
- (a) A. Li, W. Liang and R. Hughes, *J. Membr. Sci.*, 1998, **149**, 259; (b) Y. M. Lin and M. H. Rei, *Sep. Purif. Technol.*, 2001, **25**, 87; (c) E. Kikuchi, *Catal. Today*, 2000, **56**, 97.
- (a) T. Skoskiewicz, *Phys. Status Solidi A*, 1972, **11**, K123; (b) T. Skoskiewicz, *Phys. Status Solidi B*, 1973, **59**, 329; (c) B. Stritzker and W. Buckel, *Z. Phys.*, 1972, **257**, 1; (d) T. Skoskiewicz, A. W. Szafranski, W. Bujnowski and B. Baranoski, *J. Phys. C: Solid State Phys.*, 1974, **7**, 2670.
- (a) F. J. Ibanez and F. P. Zamborini, *J. Am. Chem. Soc.*, 2008, **130**, 622; (b) Y. Im, C. Lee, R. P. Vasquez, M. A. Bangar, N. V. Myung, E. R. Menke, R. M. Penner and M. H. Yun, *Small*, 2006, **2**, 356; (c) C. Langhammer, I. Zori, B. Kasemo and B. M. Clemens, *Nano Lett.*, 2007, **7**, 3122.
- (a) A. Maeland and T. B. Flanagan, *J. Phys. Chem.*, 1964, **68**, 1419; (b) A. J. Maeland and T. R. P. Gibbs, Jr., *J. Phys. Chem.*, 1961, **65**, 1270; (c) P. C. Aben and W. G. Burgers, *Trans. Faraday Soc.*, 1962, **58**, 1989; (d) T. B. Flanagan and W. A. Oates, *Annu. Rev. Mater. Sci.*, 1991, **21**, 269; (e) J. E. Schirber and B. Morosin, *Phys. Rev. B*, 1975, **12**, 117.
- S. A. Semiletov, R. V. Baranova, Y. Khodyrev and R. Imamov, *Sov. Phys. Crystallogr. (Engl. Transl.)*, 1980, **25**, 665.
- (a) A. Rose, S. Maniguet, R. J. Mathew, C. Slater, J. Yao and A. E. Russell, *Phys. Chem. Chem. Phys.*, 2003, **5**, 3220; (b) A. Czerwinski, I. Kiersztyn, M. Grden and J. Czaplá, *J. Electroanal. Chem.*, 1999, **471**, 190; (c) M. Bernardini, N. Comisso, M. Fabrizio, G. Mengoli and A. Randi, *J. Electroanal. Chem.*, 1998, **453**, 221; (d) M. C. F. Oliveira, *Electrochem. Commun.*, 2006, **8**, 647.
- M. F. Lengke, M. E. Fleet and G. Southam, *Langmuir*, 2007, **23**, 8982.
- D. W. Murphy, S. M. Zahurak, B. Vyas, M. Thomas, M. E. Badding and W. C. Fang, *Chem. Mater.*, 1993, **5**, 767.
- (a) C. P. Balde, B. P. C. Hereijgers, J. H. Bitter and K. P. de Jong, *J. Am. Chem. Soc.*, 2008, **130**, 6761; (b) K. F. Aguey-Zinsou and J. R. Ares-Fernandez, *Chem. Mater.*, 2008, **20**, 376; (c) L. Zaluski, A. Zaluska and J. O. Strom-Olsen, *J. Alloys Compd.*, 1997, **253–254**, 70; (d) V. Berube, G. Radtke, M. Dresselhaus and G. Chen, *Int. J. Energy Res.*, 2007, **31**, 637.
- M. Yamauchi, R. Ikeda, H. Kitagawa and M. Takata, *J. Phys. Chem. C*, 2008, **112**, 3294.
- (a) F. Dawood and R. E. Schaak, *J. Am. Chem. Soc.*, 2009, **131**, 424; (b) Y. Vasquez, Z. P. Luo and R. E. Schaak, *J. Am. Chem. Soc.*, 2008, **130**, 11866.
- (a) F. Fievet, J. P. Lagier, B. Blin, B. Beaudoin and M. Figlarz, *Solid State Ionics*, 1989, **32/33**, 198; (b) C. Ducamp-Sanguesa, R. Herrera-Urbina and M. Figlarz, *Solid State Ionics*, 1993, **63–65**, 25; (c) B. Wiley, Y. Sun and Y. Xia, *Acc. Chem. Res.*, 2007, **40**, 1067; (d) Y. N. Xia, Y. J. Xiong, B. K. Lim and S. E. Skrabalak, *Angew. Chem., Int. Ed.*, 2009, **48**, 60.
- Y. J. Xiong, J. Chen, B. Wiley, Y. Xia, S. Aloni and Y. Yin, *J. Am. Chem. Soc.*, 2005, **127**, 7332.
- Pearson's Handbook: Crystallographic Data for Intermetallic Phases*, ed. P. Villars, ASM International, Materials Park, OH, USA, 1997.
- A. K. Sra and R. E. Schaak, *J. Am. Chem. Soc.*, 2004, **126**, 6667.
- (a) Y. J. Xiong, J. M. McLellan, J. Y. Chen, Y. D. Yin, Z. H. Li and Y. N. Xia, *J. Am. Chem. Soc.*, 2005, **127**, 17118; (b) Y. J. Xiong, H. G. Cai, B. J. Wiley, J. G. Wang, M. J. Kim and Y. N. Xia, *J. Am. Chem. Soc.*, 2007, **129**, 3665.